Raman spectroscopy characterization of Li_2CaHfF_8 crystals

1999 J. Phys.: Condens. Matter 11 5343

(http://iopscience.iop.org/0953-8984/11/27/310)

J. Phys.: Condens. Matter **11** (1999) 5343–5354. Printed in the UK PII: S0953-8984(99)01358-2

Raman spectroscopy characterization of Li_2CaHfF_8 crystals

A P Ayala†, I Guedes†, P T C Freire†, J M Sasaki†, F E A Melo†, J Mendes Filho† and J-Y Gesland‡

† Departamento de Física, Universidade Federal do Ceará, CP 6030, 60455-760 Fortaleza (CE), Brazil

‡ Université du Maine, Cristallogenese, 72025 Le Mans Cédex 09, France

Received 28 January 1999, in final form 12 May 1999

Abstract. In this work we have presented a spectroscopic study carried out to determine the crystal structure of Li_2CaHfF_8 crystals. From x-ray, Raman and dielectric measurements we were able to identify the crystal structure of Li_2CaHfF_8 as belonging to the space group $I\bar{4}$ (S_4^2) with two molecules per unit cell. To support this identification we have analysed the correlation among the vibrational modes of Li_2CaHfF_8, $LiYF_4$ and $LiLnF_4$ (Ln: lanthanides), whose structures are body-centred tetragonal, belonging to the space group $I4_1/a$ (C_{4h}^6) with four molecules per unit cell.

1. Introduction

The search for new solid-state laser materials has attracted much interest in the last few years. Among these materials, fluorine scheelite compounds ($LiMF_4$) have been particularly widely studied since they are efficient laser hosts and find application in other optical devices. The first isomorphic fluoride studied was $LiYF_4$ [1]. Its crystalline structure is isomorphic with that of scheelite ($CaWO_4$), which belongs to the $I4_1/a$ (C_{4h}^6) space group with four molecules per unit cell [2]. In the isomorphism between $LiYF_4$ and $CaWO_4$, Li^+ corresponds to W^{4+} and Y^{3+} to Ca^{2+}. The 36 vibrational modes at the centre of the Brillouin zone are distributed among the irreducible representations of the point group C_{4h} as follows [3]:

$$\Gamma = 3A_g + 5B_g + 5E_g + 5A_u + 3B_u + 5E_u$$

where one A_u mode and one E_u mode correspond to rigid translations of the whole crystal. The other A_u and E_u modes are infrared active while the g modes are Raman active. The phonons of B_u symmetry are neither Raman nor infrared active.

Several studies have already been reported concerning the spectroscopy characterization of $LiMF_4$ compounds [4–12]. For instance Salaün *et al* [10] studied the lattice dynamics of the fluoride scheelites $LiYF_4$ and $LiLnF_4$ (Ln = Ho, Er, Tm and Yb) by means of Raman, infrared and inelastic neutron scattering, while Zhang *et al* [9] studied, by means of Raman spectroscopy, the crystalline structure of $LiGdF_4$. Besides this class of fluorine compounds, other families of fluoride scheelites have also been studied. In 1973, Védrine *et al* [13] presented a new family of fluoride scheelites where the yttrium ions are replaced by both a bivalent element (M^{II} = Ca, Cd) and a tetravalent one (M^{IV} = Th, U, Ce, Tb, Zr, Hf), producing $Li(M_{0.5}^{II}M_{0.5}^{IV})F_4$-type compounds. On the basis of powder crystallographic investigation, the authors suggested that the structure of these compounds is related to that of scheelite $LiYF_4$, as they were able to establish a 1–1 order between M^{II} and M^{IV} atoms. This means that some reflections which are forbidden for the basic scheelite structure are now

observed. Hence a double molecule is necessary for describing this structure, i.e. $Li_2M^{II}M^{IV}F_8$. Somewhat later, Védrine *et al* [15] presented a paper reporting a careful x-ray investigation of Li_2CaUF_8 crystal. According to their results, Li_2CaUF_8 has a body-centred-tetragonal structure belonging to the space group $I\bar{4}m2$ (D^9_{2d}). The unit cell, with lattice parameters $a = 5.2290(12)$ Å and $c = 11.0130(18)$ Å, contains two formula units. In this structure, the sublattice formed by Li, Ca and U cations is equivalent to that of $LiYF_4$, where Ca and U are placed at the Y sites. The most important difference is found in the fluorine distribution, where the number of sites is doubled, each one being half-occupied. In view of the presence of intrinsic fluorine vacancies, the authors suggest that if the disorder is dynamic, a high ionic conductivity would be observed along the tetragonal axis. Thus the structure presents possible conduction channels in this direction.

To the best of our knowledge, no one has reported on the Raman investigation of this family. Hence, the main purpose of this work is to identify the crystalline structure of Li_2CaHfF_8 using x-ray, Raman and dielectric measurements. Through the use of these techniques we were able to determine the crystal structure of Li_2CaHfF_8 as body-centred tetragonal, belonging to space group $I\bar{4}$ (S^2_4) with two molecules per unit cell. To verify this finding, we have performed an analysis of the correlation between the vibrational modes of Li_2CaHfF_8 and $LiYF_4$, $LiLnF_4$ (Ln: lanthanides) crystals.

2. Experimental procedure

In spite of an incongruent melting, single crystals of Li_2CaHfF_8 several cm^3 in size have been pulled from stoichiometric melts using the Czochralski technique.

Raman spectra were recorded in backscattering geometry using a micro-Raman instrument. The spectrometer used was a Jobin–Yvon T64000 Raman system equipped with an Olympus BX40 microscope and a N_2-cooled charge-coupled device (CCD). The scattering was excited with the 514.5 nm line of an Ar-ion laser. All measurements were performed using a long-working-distance planar achromatic objective (20×/0.35, 20.5 mm) to avoid the propagation of oblique phonons. The scattering geometries for the spectra listed in the text and figures follow the usual Porto notation, $A(BC)D$ [16].

The x-ray diffraction pattern was obtained using a Rigaku powder diffractometer operating with Cu Kα radiation at 40 kV/25 mA at room temperature. The x-ray pattern was taken in the stepping scan mode with five seconds of counting time for each step of 0.01°.

3. Results

3.1. X-ray diffraction

The x-ray powder diffraction pattern of Li_2CaHfF_8 obtained at room temperature is shown in figure 1. This diagram can be indexed by reference to a body-centred-tetragonal cell with $a = 5.1035(3)$ Å and $c = 10.5170(8)$ Å, in agreement with the observations of Védrine *et al* [13]. By comparing these cell dimensions with those of $LiYF_4$ [14] and $LiLnF_4$ [17], a similar structure can be predicted for Li_2CaHfF_8 crystals. However, although all reflections in this pattern are compatible with the condition $h + k + l = 2n$, the additional conditions of the $LiYF_4$ space group ($hk0$: $h, k = 2n$ and $00l$: $l = 4n$) are not satisfied, leading to a structure different to that proposed by Védrine *et al* for Li_2CaUF_8 [15].

To reduce the number of possible space groups, we have performed complex impedance spectroscopy. From these measurements we observed the appearance of several piezoelectric resonances—which indicates that the crystal structure is non-centrosymmetic—and that the

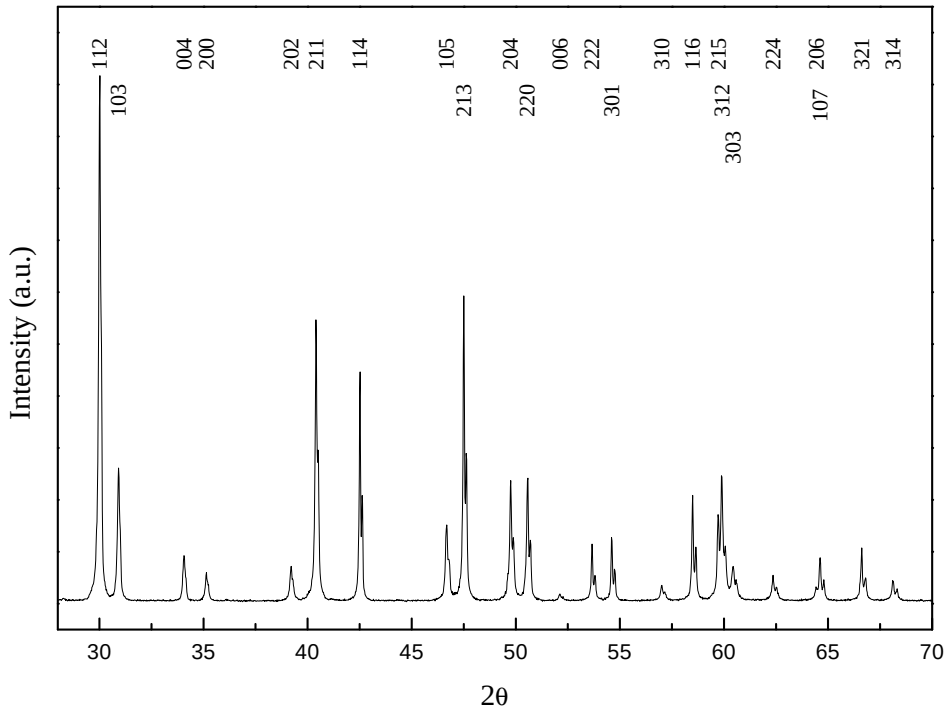

Figure 1. An x-ray diffractogram of Li_2CaHfF_8.

value of the electrical conductivity at 500 °C measured along the tetragonal-axis direction is $10^{-8}\ \Omega^{-1}\ cm^{-1}$, which is a very low value for fluoride ionic conductors [18, 19]. This latter result states that the fluorine-ion sites in the Li_2CaHfF_8 structure must be completely occupied in contrast to the fluorine-ion-site distribution in the Li_2CaHfF_8 structure proposed by Védrine *et al* [15].

While the fluoride scheelites have four molecules per unit cell, $Li_2(M^{II}M^{IV})F_8$ compounds have only two. In consequence, we seek space groups that have two sites with multiplicity two, for Hf and Ca ions. Among the non-centrosymmetric tetragonal body-centred space groups, only five satisfy these conditions, namely $I4$, $I\bar{4}$, $I\bar{4}2m$, $I\bar{4}m2$ and $I4mm$. Since the central Li ion and the Li ion placed on the face of the $LiYF_4$ cell are related to each other by the inversion centre, it is possible that there are two non-equivalent Li ions in non-centrosymmetric Li_2CaHfF_8. Thus, two more sites of multiplicity two are needed to describe this crystal. With this condition, the list of possible space groups is reduced to $I\bar{4}$ (S_4^2) and $I\bar{4}2m$ (D_{2d}^9). By comparing the possible atomic sites in the proposed space groups, we observe that the sublattice of Li, Hf and Ca ions is the same for both groups. Thus, the fundamental difference between them will be determined by the fluorine distribution.

3.2. Group theory predictions

To decide which is the correct space group for Li_2CaHfF_8 crystal, we will analyse Raman spectra in the light of the irreducible representations of both groups. The irreducible representations have been obtained using the method of site group analysis proposed by Rousseau *et al* [20].

Let us assume, as proposed by Védrine *et al* [15], that the crystal belongs to the $I\bar{4}m2$ (D^9_{2d}) space group. In this case, the ions can be positioned at the following sites:

$$\infty[jC_1(16)] + \infty[iC_2(8)] + \infty[(h+g)C_2(8)] + \infty[(f+e)C_{2v}(4)] + (d+c+b+a)D_{2d}(2).$$

Table 1 lists the vibrational modes generated by particular atoms in an elementary cell of Li_2CaUF_8 as proposed by Védrine *et al* [15]. In this representation, A_2 modes are silent, while the other modes are Raman active and correspond to the following components of the Raman polarizability tensor:

A_1: $\alpha_{xx} + \alpha_{yy}, \alpha_{zz}$

B_1: $\alpha_{xx} - \alpha_{yy}$

B_2: α^z_{xy}

E: $\alpha^y_{xz}, \alpha^x_{yz}$.

Table 1. Site symmetries of atoms and vibrational modes in the D^9_{2d} space group.

Atom	Site symmetry	Number of vibrations				
		A_1	A_2	B_1	B_2	E
Li^1	D_{2d}				1	1
Li^2	D_{2d}				1	1
Ca	D_{2d}				1	1
Hf	D_{2d}				1	1
F^1	C_1	3	3	3	3	6
F^2	C_1	3	3	3	3	6

Total: $\Gamma = 6A_1 + 6A_2 + 6B_1 + 10B_2 + 16E$

Acoustic: $\Gamma_{ac} = B_2 + E$

Vibrational: $\Gamma_{vib} = 6A_1 + 6A_2 + 6B_1 + 9B_2 + 15E$

From different scattering geometries, we can see that pure A_1 modes are observed in the $x(zz)\bar{x}$ geometry or mixed with B_1 modes in the $x(yy)\bar{x}$ and $z(xx)\bar{z}$ geometries. B_2(LO) modes are active only in the $z(xy)\bar{z}$ geometry while a mixture of E(TO) and E(LO) modes are observed in the $x(yz)\bar{x}$ configuration.

For the $I\bar{4}$ (S^2_4) space group, the ions in Li_2CaHfF_8 can be distributed over the following sites:

$$\infty[gC_1(8)] + \infty[(f+e)C_2(4)] + (d+c+b+a)S_4(2).$$

The irreducible representation for this space group is presented in table 2. All vibrational modes of the S_4 factor group are Raman active with the following components of the Raman polarizability tensor:

A: $\alpha_{xx} + \alpha_{yy}, \alpha_{zz}$

B: $\alpha^z_{xx} - \alpha^z_{yy}, \alpha^z_{xy}$

E: $\begin{cases} \alpha^x_{xz}, \alpha^y_{yz} \\ \alpha^y_{xz}, \alpha^x_{yz}. \end{cases}$

Thus, A modes are observed in the $x(zz)\bar{x}$ geometry. B(LO) modes are active in the $z(xy)\bar{z}$ configuration while B(LO) and A modes are mixed in the $z(xx)\bar{z}$ geometry. B(TO) modes are mixed with A modes in the $x(yy)\bar{x}$ geometry. Finally, a mixture of E(TO) and E(LO) modes is observed in the $x(yz)\bar{x}$ scattering geometry.

Table 2. Site symmetries of atoms and the vibrational modes in the S_4 space group.

Atom	Site symmetry	Number of vibrations A	B	E
Li^1	S_4		1	1
Li^2	S_4		1	1
Ca	S_4		1	1
Hf	S_4		1	1
F^1	C_1	3	3	3
F^2	C_1	3	3	3

Total: $\Gamma = 6A + 10B + 10E$
Acoustic: $\Gamma_{ac} = B + E$
Vibrational:$\Gamma_{vib} = 6A + 9B + 9E$

3.3. Raman spectroscopy

Raman spectra for each scattering geometry described in the previous section are shown in figure 2. In figure 2(a) six vibrational modes are observed. Two very low-intensity peaks are shown in the inset. To detect them an average of many long-time spectra was used. To simplify the figures, only the phonon frequency of the low-intensity peaks is indicated. Deconvolution of overlapping bands was performed by using a non-linear least-squares fit assuming Lorentzian line profiles. As a rule, the frequency of the bands due to a slight misalignment in the crystal orientation is shown in parentheses. The other scattering geometries exhibit (b) 11 modes ($z(xx)\bar{z}$), (c) 10 modes ($z(xy)\bar{z}$), (d) 10 modes ($x(yy)\bar{x}$) and (e) 16 modes ($x(yz)\bar{x}$).

Now let us analyse the Raman spectra on the basis of the group theory analysis, in order to provide the correct space group for the Li_2CaHfF_8 structure. First, we analyse these spectra in terms of the D_{2d} factor group. The $x(zz)\bar{x}$ spectrum shows six modes, which agrees with the group theory predictions and can be associated with A_1 modes. A similar situation is found in the $z(xy)\bar{z}$ geometry where the nine B_2(LO) phonons predicted are observed. However, the other configurations show some discrepancies. The $z(xx)\bar{z}$ and the $x(yy)\bar{x}$ scattering geometries should show the same number of vibrational modes, i.e. $6A_1 + 6B_1$. However, after discounting the A_1 modes observed in the $x(zz)\bar{x}$ spectrum, eight lines remain in the $z(xx)\bar{z}$ and the $x(yy)\bar{x}$ spectra—more lines remain than the $6B_1$ predicted by group theory. Furthermore, a considerable frequency shift of many non-polar B_1 modes between these spectra can be observed, suggesting a TO–LO splitting. Another interesting point is that there is a great similarity between the $z(xx)\bar{z}$ and the $z(xy)\bar{z}$ spectra, where we should observe the B_1 and the B_2 modes respectively. Finally, both TO and LO components of the E modes are active in $x(yz)\bar{x}$ geometry, giving rise to a complex spectrum. These results suggest that the Raman spectra observed cannot be associated with D_{2d} factor group mode distribution.

By considering the S_4 factor group distribution, the six phonons found in the $x(zz)\bar{x}$ spectrum are seen to correspond to A modes. In the $z(xx)\bar{z}$ geometry, nine B(LO) modes are identified, while in the $z(xx)\bar{z}$ geometry, the same modes are observed together with A modes. The shift of B modes observed in the $x(yy)\bar{x}$ geometry is due to the presence of non-polar active A modes with B(TO) modes. Again, E modes do not yield relevant information as regards the choice of the correct factor group, because 9E(TO) + 9E(LO) modes is the prediction while only 15 modes are observed in $x(yz)\bar{x}$ geometry.

Since our Raman scattering spectra can be interpreted in full on the basis of the S_4 factor group, we propose $I\bar{4}$ as the most probable space group for Li_2CaHfF_8 crystal. The list of

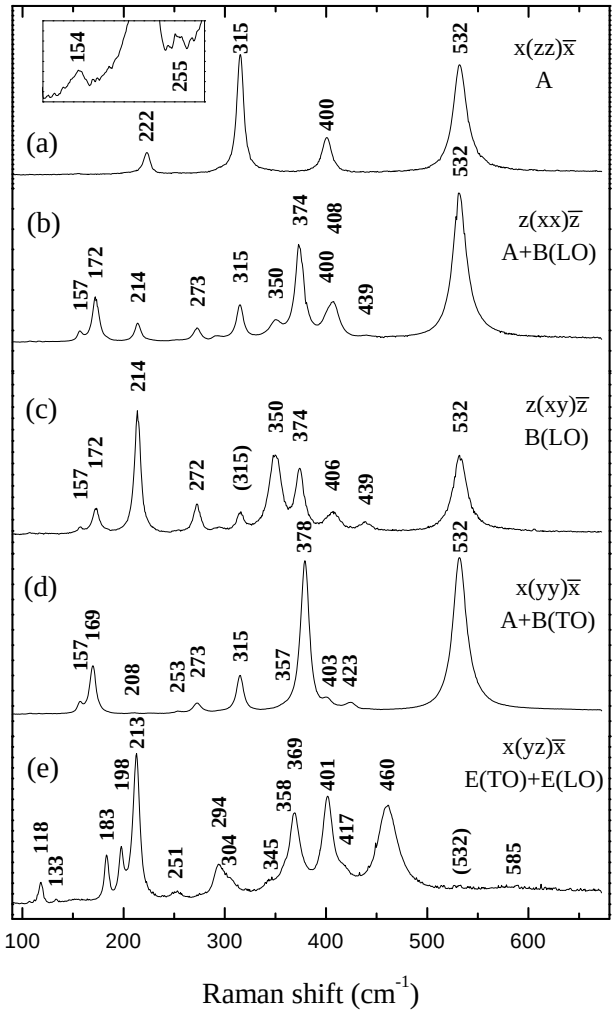

Figure 2. Raman spectra of Li_2CaHfF_8 for different scattering geometries. The lines attributed to polarization leaks are in parentheses.

observed vibrational modes is given in table 3, while the choice of the order of the B(TO) phonons will be explained in the next section.

4. Discussion

To support our labelling of the space group of Li_2CaHfF_8 crystal, we present a study of the correlation between the vibrational modes observed in this crystal and those observed in $LiLnF_4$ (Ln: lanthanides) crystals which belong to space group C_{4h}, as a function of the square root of the reciprocal cationic mass. We intend to explain how the vibrational modes belonging to C_{4h} are transformed when we replace Y or Ln ions by Ca and Hf giving rise to the S_4 space group. It should be noted that if the fluorine ions occupy only one general position in the D_{2d} group, all of them will be completely filled. However, as can be inferred from table 1, only three A_1 modes would be observed in the $x(zz)\bar{x}$ geometry, contrary to our experimental results.

Table 3. Vibrational modes observed in Li_2CaHfF_8.

A	154	222	255	315	400	532			
B(LO)	157	172	214	273	350	374	408	439	532
B(TO)	157	169	208	253	273	357	403	423	378
E(LO) + E(TO)	118	133	183	197	212	251	293	304	345
	358	369	401	417	461	585			

Several sets of experimental data from Raman scattering and infrared spectroscopy have been reported for $LiYF_4$ and $LiLnF_4$ (Ln = Gd, Tb, Dy, Ho, Er, Tm, Yb and Lu) [4–12] crystals. In $CaWO_4$ isomorphous crystals, the internal vibrations of WO_4^{2-} dominate the spectra and are little shifted from the free-ion frequencies. For $LiYF_4$, as pointed out by Miller *et al* [4],

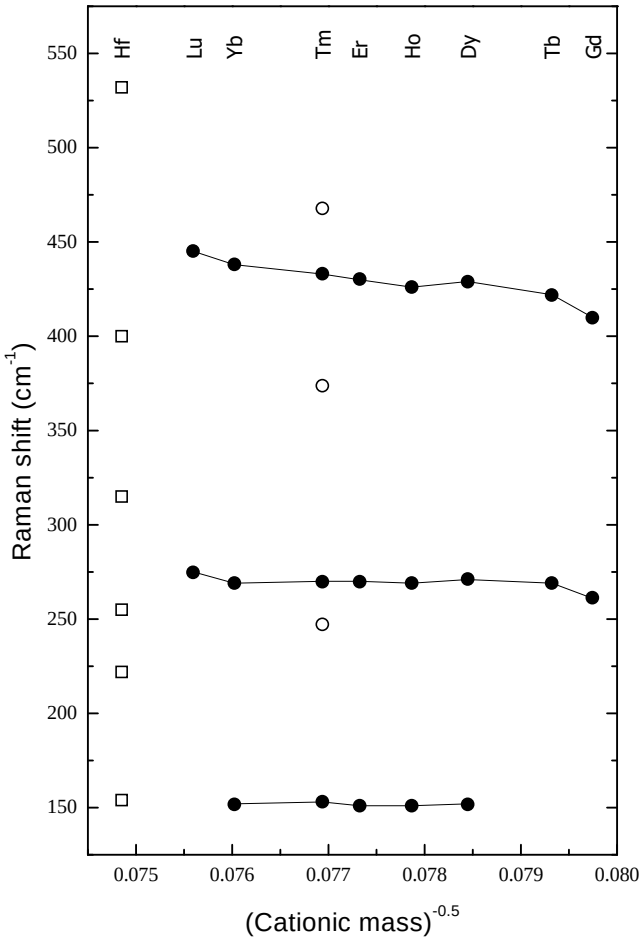

Figure 3. Li_2CaHfF_8 A (□) and $LiLnF_4$ A_g (●) and B_u (○) vibrational modes as functions of the square roots of the reciprocal masses of the heavy cations.

the internal binding of the LiF_4^{3-} tetrahedra is not significantly different from the other ionic forces in the crystal; thus the internal and external vibrations are not well separated in the Raman spectra. However, they define a set of 'basis' modes in terms of symmetry coordinates, which transforms according to the irreducible representations of the point group. Salaün *et al* carried out a detailed study of the $LiYF_4$ and $LiLnF_4$ vibrational spectra using Raman, infrared and inelastic neutron scattering [10, 11]. With these results and using a rigid-ion model, they calculated the main components of the eigenvectors of the Raman- and IR-active modes and identified them as the base modes defined by Miller *et al* [4]. Using this framework, we will compare the vibrational modes measured for Li_2CaHfF_8 with the results of Salaün *et al* for $LiYF_4$ and $LiLnF_4$ (Raman and IR, Ln = Ho, Er, Tm and Yb) [10], Zhang *et al* for $LiGdF_4$(Raman) [9], Dörfler and Schaack for $LiTbF_4$ (Raman and IR) [7] and Kupchikov *et al* for $LiLnF_4$ (Raman, Ln = Dy and Lu) [12].

To compare the vibrational modes of Li_2CaHfF_8 with those of $LiYF_4$ and $LiLnF_4$, we need to determine the relationship between the S_4 and C_{4h} point groups. Since S_4 is a subgroup of C_{4h} generated by missing out the inversion centre, A modes result from the combination of

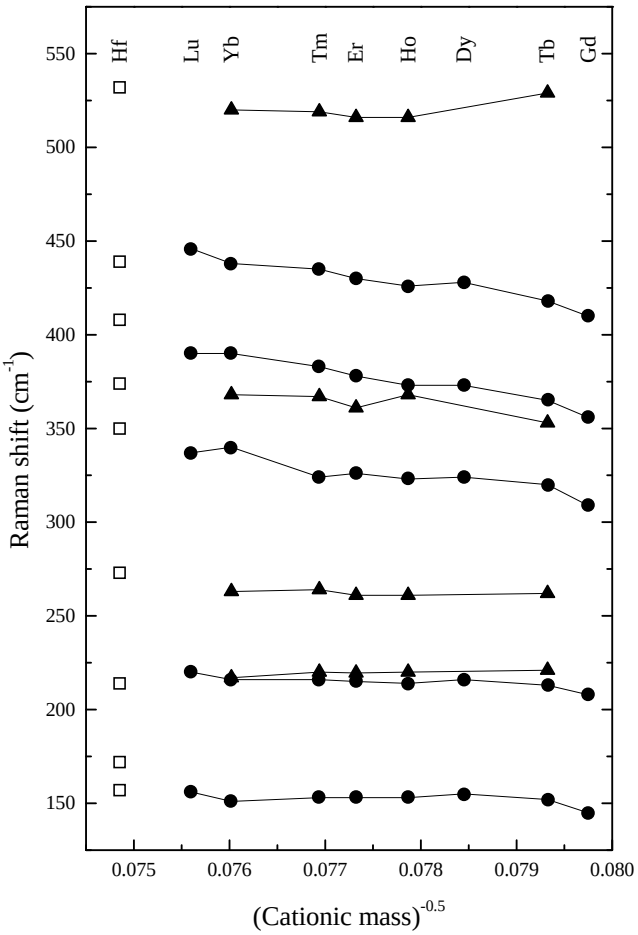

Figure 4. Li_2CaHfF_8 B(LO) (□) and $LiLnF_4$ B_g (●) and A_u(LO) (▲) vibrational modes as functions of the square roots of the reciprocal masses of the heavy cations.

A_g and B_u modes, B modes result from the combination of A_u and B_g modes, and E modes come from the mixing between E_g and E_u modes [20]. Furthermore, modes that are silent or infrared active are now observed in Raman spectra.

In figure 3 we plot the frequencies of the A_g modes of some lanthanide fluoride scheelites as functions of the square roots of the reciprocal masses of the heavy cations. In the same figure we include A modes measured for the Li_2CaHfF_8 crystal in the column corresponding to the hafnium mass. This choice is justified by the fact that Hf ion is 4.5 times heavier than calcium and its weight is close to that of lanthanide ions. We did not include the $LiYF_4$ vibrations since yttrium is two times lighter than the lanthanides. Since B_u modes are silent, the only available information about them was obtained by rigid-ion-model calculations for $LiTmF_4$ by Kupchikov *et al* [6]. In this figure we show that only the lowest phonon frequencies of the A_g and A representations have a clear correlation. These modes represent the z-rotation of the LiF_4^{3-} tetrahedra [11], since only the fluorine ions are involved in the A representation (table 1). While we measure a very intense A mode at high frequency, among the A_g phonons of the lanthanide fluoride scheelites, the only intense mode is in the intermediate region ($\sim$265 cm^{-1}),

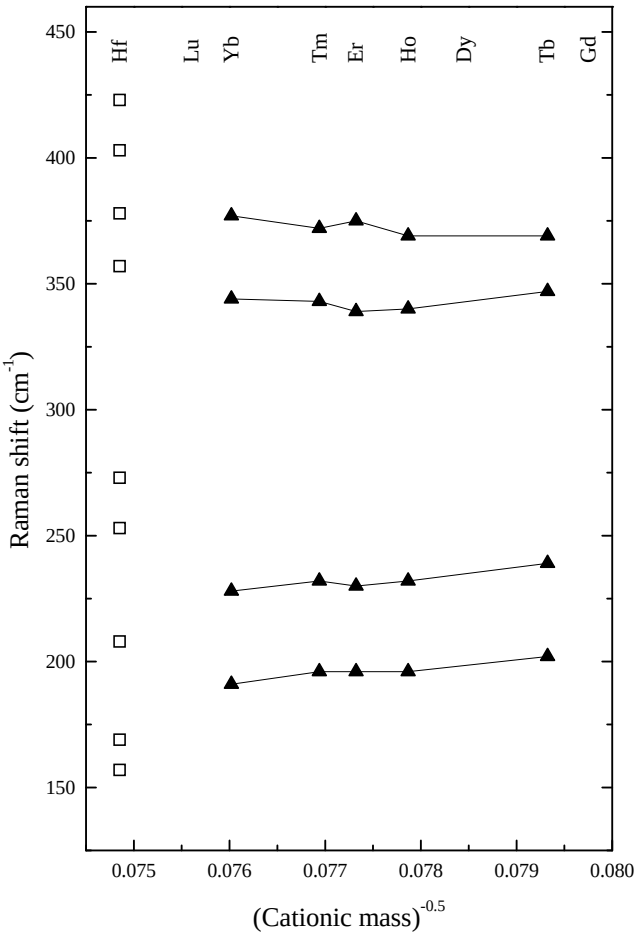

Figure 5. Li_2CaHfF_8 B(TO) (□) and $LiLnF_4$ A_u(TO) (▲) vibrational modes as functions of the square roots of the reciprocal masses of the heavy cations.

whereas the other A_g modes are very weak [10]. This indicates that the high-frequency A mode should be related to a B_u mode that is silent in C_{4h}, as indicated by the calculations made by Kupchikov *et al*.

In figure 4 we plot B(LO) and A_u(LO) + B_g modes, while in figure 5 the B(TO) mode frequencies are plotted together with the A_u(TO) ones. There are three regions from which we can identify an evident relationship between $LiLnF_4$ and Li_2CaHfF_8 vibrational modes. According to calculations made by Salaün *et al* these regions are:

(a) 0–200 cm^{-1}, where the vibrations are essentially due to the motions of the YF_8 double tetrahedra,
(b) 400 to 600 cm^{-1}, where the vibrations are determined by the LiF_4 tetrahedra and
(c) 200 to 400 cm^{-1}, where the vibrations are essentially those of the fluorine ions.

In figure 4, we can observe that the A_u(LO) and B_g phonons of the two upper regions are directly related to the Li_2CaHfF_8 B(LO) modes. In the lowest region, dominated by the heaviest ions, the relationship is less evident, due possibly to the presence of two different double tetrahedra

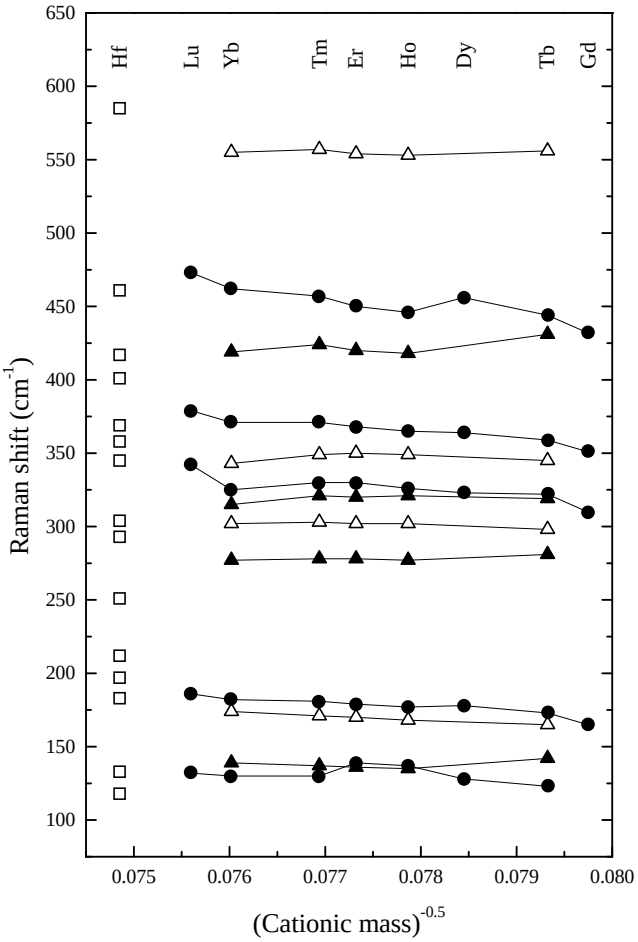

Figure 6. Li_2CaHfF_8 E(TO) and E(LO) (□) and $LiLnF_4$ E_g (●), E_u(TO) (▲) and E_g (△) modes as functions of the square roots of the reciprocal masses of the heavy cations.

in Li_2CaHfF_8 (HfF_8 and CaF_8). Note that non-polar B_g modes transform into polar B modes, so a TO–LO splitting can be expected. By comparing the TO and LO A_u phonons measured for $LiLnF_4$ and the phonons of Li_2CaHfF_8, we can provide an identification of the TO–LO splitting for B phonons. We can suppose that, due to the similarities between the two structures (cell dimensions and atomic distributions), the TO–LO splitting of polar A_u phonons is not very much affected by the loss of the inversion centre. Using this and the fact that the TO frequency is always lower than the LO frequency, we can propose the phonon distribution presented in table 3.

Finally, $E_g + E_u(TO) + E_u(LO)$ modes together with E(TO) + E(LO) modes are shown in figure 6. The frequency regions described by Salaün *et al* [11] are clearly identified among the $LiLnF_4$ vibrational modes. This is more difficult for Li_2CaHfF_8, because the non-polar E_g modes split into E(TO) and E(LO). Furthermore, the substitution for lanthanides with hafnium (heavier) and calcium (lighter) produces a broadening of the lower region (as stated by Salaün *et al*). By using arguments similar to those put forward for the B mode case, we could identify the TO–LO splitting of E modes. However, since the separation of TO and LO components of E modes in the S_4 factor group is not possible from Raman spectra, any association could be merely speculative.

5. Conclusions

The analysis of our results allows us to propose the space group $I\bar{4}$ (S_4^2) for Li_2CaHfF_8 crystal. Raman scattering measurements agree well with the group theory analysis. In addition, our classification is supported by the clear relationship observed between the Li_2CaHfF_8 and the $LiLnF_4$ phonons, which is predicted on the basis of the correlation between the C_{4h} and S_4 factor groups. An other interesting result is that all fluorine sites are fully occupied, in contrast to the case for the structure of Li_2CaUF_8 proposed by Védrine *et al* [15]. This fact is compatible with the low ionic conductivity in the z-direction observed in Li_2CaHfF_8 crystals.

Acknowledgments

We thank Professor Roberto Luiz Moreira for his help with the complex impedance spectroscopy measurements. This work was partially supported by the Brazilian agencies CNPq and FUNCAP.

References

[1] Thoma R E, Wearer C F, Insley H, Harris L A and Yarkel H A Jr 1961 *J. Phys. C: Solid State Phys.* **65** 1096
[2] Wyckoff R W G 1964 *Crystal Structures* 2nd edn, vol 3 (New York: Interscience) p 19ff
[3] Borber A S Jr 1964 *Phys. Rev.* **135** A742
[4] Miller S A, Rast H E and Caspers H H 1970 *J. Chem. Phys.* **52** 4172
[5] Korableva S L, Kupchikov A K, Petrova M A and Ryskin A I 1980 *Sov. Phys.–Solid State* **22** 1115
[6] Kupchikov A K, Malkin B Z, Rzaev D A and Ryskin A I 1982 *Sov. Phys.–Solid State* **24** 1348
[7] Dörfler W and Schaack G 1985 *Z. Phys.* B **59** 283
[8] Schultheiss E, Scharmann A and Schwabe D 1986 *Phys. Status Solidi* b **138** 465
[9] Zhang X X, Schulte A and Chai B H T 1994 *Solid State Commun.* **89** 181
[10] Salaün S, Fornoni M T, Bulou A, Rousseau M, Simon P and Gesland J Y 1997 *J. Phys.: Condens. Matter* **9** 6941
[11] Salaün S, Bulou A, Rousseau M, Hennion B and Gesland J Y 1997 *J. Phys.: Condens. Matter* **9** 6957
[12] Kupchikov A K, Malkin B Z, Natadze A L and Ryskin I 1987 *Sov. Phys.–Solid State* **29** 1913
[13] Védrine A, Baraduc L and Cousseins J-C 1973 *Mater. Res. Bull.* **8** 581
[14] Garcia E and Ryan R R 1993 *Acta Crystallogr.* C **49** 2053

[15] Védrine A, Trottier D, Cousseins J C and Chevalier R 1979 *Mater. Res. Bull.* **14** 583
[16] Porto S P S and Scott J F 1967 *Phys. Rev.* **157** 716
[17] *Landolt–Börnstein New Series* 1973 Group III, vol 7 (Berlin: Springer)
[18] Chandra S 1998 *Superionic Solids—Principles and Applications* (Amsterdam: North-Holland) p 118ff
[19] Ayala A P, Oliveira M A S, Gesland J-Y and Moreira R L 1998 *J. Phys.: Condens. Matter* **10** 5161
[20] Rousseau D L, Bauman R P and Porto S P S 1981 *J. Raman Spectrosc.* **10** 253